JAAS

Cite this: *J. Anal. At. Spectrom.*, 2012, **27**, 604

www.rsc.org/jaas

PAPER

Effect of a mass spectrometer interface on inductively coupled plasma characteristics: a computational study

Maryam Aghaei,* Helmut Lindner and Annemie Bogaerts

Received 28th November 2011, Accepted 17th January 2012
DOI: 10.1039/c2ja10341a

An inductively coupled plasma connected to a mass spectrometer interface (sampling cone) is computationally investigated. Typical plasma characteristics, such as gas flow velocity, plasma temperature and electron density, are calculated in two dimensions (cylindrical symmetry) and compared with and without a mass spectrometer sampling interface. The results obtained from our model compare favorably with experimental data reported in the literature. A dramatic increase in the plasma velocity is reported in the region close to the interface. Furthermore, a cooled metal interface lowers the plasma temperature and electron density on the axial channel very close to the sampling cone but the corresponding values in the off axial regions are increased. Therefore, the effect of the interface strongly depends on the measurement position. It is shown that even a small shift from the actual position of the sampler leads to a considerable change of the results.

1. Introduction

Inductively coupled plasma (ICP) has become the most popular source in analytical chemistry for both atomic emission spectrometry (AES) and mass spectrometry (MS).[1–3] Because of the many similarities between the ICPs used for AES and MS, researchers have used the reported fundamental characteristics of ICP emission sources to understand the performance of elemental mass spectrometers that use the ICP as an ion source.[4] However, in ICP-MS, representative samples of the plasma should be transmitted through an orifice (*i.e.*, the so-called "sampler") to the mass analyzer. It can be expected that the insertion of a metal cone interface, which is grounded and cooled, into the high temperature plasma causes changes in the plasma characteristics that affect the analytical performance of ICP-MS. Because ICP-MS is one of the most important techniques for elemental analysis,[5] this effect of the sampling interface should be investigated in more detail.

In the literature, a lot of studies have reported on ICP characteristics in the presence of a MS sampling interface. Many studies focused on the downstream region from the interface [*e.g.*, ref. 6–9], but did not give information on changes in the plasma itself. In ref. 10–18, the upstream region, *i.e.*, the plasma, was investigated, but no comparison was made with and without the sampling interface. Only Hieftje and group members[19] and Farnsworth and coworkers[4] have made a detailed comparison of the plasma characteristics with and without the sampling interface. Lehn *et al.*[19] reported that the presence of the interface causes changes in the fundamental plasma characteristics such as electron number density and gas kinetic temperature, whereas Ma *et al.*[4] used laser-induced fluorescence to investigate the effect of the sampling interface on the analyte atom and ion distributions in the ICP used as an ion source for elemental mass spectrometry.

Besides experimental studies, a computational investigation can provide a better insight into how and to what extent the plasma characteristics upstream in the ICP are affected when it is coupled with a MS. Indeed, in simulations it is possible to obtain the entire two-dimensional (2D) picture, whereas in experiments the information is only obtained at specific measurement positions. It is for instance not possible to measure at the exact position of the sampling orifice, whereas such limitations do not exist for simulations.

Spencer *et al.*[20,21] applied the so-called Direct Simulation Monte Carlo (DSMC) algorithm to simulate the flow of neutral argon gas through the first vacuum stage of the ICPMS; they also presented a comprehensive review of the approximate model of ideal gas flow through the sampling cone which had been used in 1988 for the hemispherical-sink model by Douglas and French.[22] Their calculations yielded plasma velocity data in the region a few millimetres upstream from the sampler which were in reasonable agreement with experiments. They provided a formula for the Mach number as a function of distance along the central axis which may be used to predict the variation of velocity, density and temperature along the central axis near the sampler.[21] However, the model assumed the so-called uniform upstream condition which means that the upstream density and temperature gradients associated with the cool center and the hot outer region of the gas flow from the ICP torch are not included.[20] Moreover, there is no plasma assumed in the model and there is a need to provide approximate parameters at the stagnation point.

Research Group PLASMANT, Department of Chemistry, University of Antwerp, Universiteitsplein 1, B-2610 Wilrijk-Antwerp, Belgium. E-mail: Maryam.aghaei@ua.ac.be

In the present paper, the effect of the presence of a sampler on the fundamental plasma characteristics in ICPMS is computationally investigated, based on the model explained in ref. 23 and 24. To our knowledge, such a detailed computational study has not been carried out before. The calculation results will be compared with the measured data from ref. 4,10 and 19, and will provide a better insight into the underlying physics responsible for the effect of the sampling interface.

2. Description of the model

For the calculations, a commercial computational fluid dynamics (CFD) program, called Fluent v13.0.0 (ANSYS), was used.[25] The so-called coupled algorithm was employed as the solver in the simulations. To simulate the plasma behavior, some self-written modules were added as user defined functions (UDFs), as is explained in detail in ref. 23. These modules define the heat capacity and the thermal conductivity. The 2D axisymmetric geometry considered in the simulation is described in detail in ref. 23. Argon is used for the ICP gas stream, as well as the ambient gas. As discussed in ref. 23, the local thermodynamic equilibrium (LTE) condition is applied to the plasma.[26] The Reynolds number of the flow, even at the place of the sampler (=115.6), is far from the turbulence regime. Therefore, a laminar behavior can be assumed and the Navier–Stokes equations are solved to determine the flow patterns.[25] The plasma species considered in the model are Ar atoms, singly charged and doubly charged Ar ions, as well as electrons, and their transport properties are calculated by kinetic theory, as described in detail by Lindner *et al.* in ref. 23. The model is validated by experimental work in ref. 24. In the present work, a mass spectrometer interface (sampler) is added to the geometry, at the position of 10 mm above the load coil, on the center axial line. The sampler has a central orifice with 1 mm diameter (see Fig. 1b).

To investigate the effects of the sampler, two sets of calculations with exactly the same conditions, with and without the sampler, are performed. In the case without the sampler, the plasma has more space and could flow through the whole axial length (Fig. 1a). The calculation region has a radius of 10 cm and an axial length of 15 cm in the case without the sampler and 4.5 cm axial length in the case with the sampler. Note that this calculation region is much higher than the real geometry of the plasma, but this allows simpler boundary conditions, *e.g.* electric fields could be set to 0 at the boundary without affecting the plasma behavior. The total power coupled to the plasma is set to 1000 W and the frequency of the harmonic external electric current density is 27 MHz. The central gas flow rate is 1 L min^{-1} and the flow rates of the outer and intermediate torch tubes are 12 L min^{-1} and 0.4 L min^{-1}, respectively. The ambient gas pressure and exhaust pressure are set to 101 325 Pa and 101 225 Pa, respectively. In the case with the sampler, the pressure downstream of the sampler is set to 133.32 Pa.

3. Results and discussion

3.1. Flow path lines and velocity

The gas flow path lines, originating from the central and outer inlets, colored by velocity in m s^{-1}, are plotted in Fig. 1a and b, for the case without and with the sampler, respectively. The path

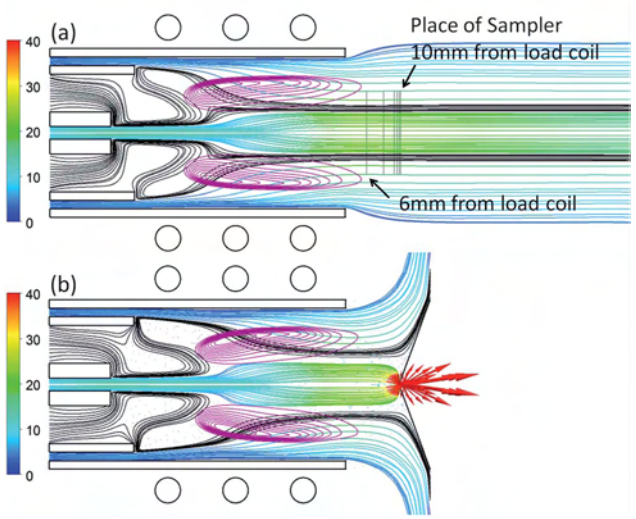

Fig. 1 2D gas flow velocity path lines originating from the central and outer inlets, colored by velocity in m s^{-1}, and from the intermediate inlet, colored in black: (a) without and (b) with the sampler. The thin vertical solid lines in (a) indicate the axial positions at which the radial profiles of Fig. 4 and 6 are plotted, *i.e.*, at 6 mm, 8 mm, 9.3 mm, 9.6 mm, 9.9 mm, and 10 mm from the load coil. Velocity vectors are also plotted in (b), when the gas is flowing through the sampling orifice. The purple contours indicate the area of external power coupling.

lines originating from the intermediate inlets are colored in black to be distinguishable from the central and outer gas, and for the sake of further discussion in Section 3.2. The orifice of the sampler is placed at 10 mm from the load coil. It is clear from both figures that the flow coming from the central inlet, instead of maintaining a straight line trajectory, adopts a curved flow profile due to the entrainment forces acting upon it, as was predicted by Stewart *et al.* to be a likely scenario for off-axis sampling of an ion cloud (Fig. 8c of ref. 10). This scenario was supported by experiments.[10] Nevertheless, in the case with the sampler (Fig. 1b), as a consequence of flow acceleration to the orifice of the sampler, the whole central flow is able to pass through the interface cone. However, the intermediate and outer flows are not affected by the acceleration process to the orifice, and they adopt a curved line trajectory to the open sides of the torch at the end sides of the interface cone. This modification of path lines affects the temperature and electron density profiles, which will be presented below.

In addition, the graphs illustrate how the gas velocity in the area close to the sampler is changed by the presence of the sampler. Indeed, a large difference in pressures upstream and downstream of the sampler (*i.e.*, 101 191.68 Pa), considering Bernoulli's principle, causes an extreme increase in the velocity of the flowing plasma, as is illustrated in Fig. 1b by the red velocity vectors in m s^{-1}, added to better visualize this effect. The same effect is apparent from Fig. 2, which shows the velocity on the central axis as a function of axial position. In both cases, *i.e.*, with and without the sampler, the velocity rises when the flow leaves the load coil (*i.e.*, around 30 mm from the injector inlet), because the gas is heated up by the power coupled to the plasma, which results in the increased velocity.[24] The effect of the sampler on the velocity is obvious from the solid line in Fig. 2, which exhibits a sharp increase towards the sampler. Note that the solid

line is plotted to 1 mm before the sampler, to fit in the *y*-scale of this figure, but the velocity increases further to about 890 m s^{-1} when it passes the sampler orifice. Ma *et al.* have also observed a similar rise in velocity due to the presence of the sampler, as reported in ref. 4.

3.2. Temperature

The plasma temperature is a fundamental property of the ICP. Indeed, temperature changes affect the plasma thermal conductivity. Moreover, the rate of droplet desolvation and particle vaporization is affected by the gas kinetic temperature.[27] Inserting a cooled metal sampler as an interface between ICP and the mass spectrometer causes the following changes, as presented in Fig. 3–5.

The 2D profiles of the plasma temperature are presented in Fig. 3, both in the absence (Fig. 3a) and presence (Fig. 3b) of the mass spectrometer interface. It is clear that the off-axial region of the plasma has a higher temperature than the central region in both Fig. 3a and b, which indicates the presence of the central channel cooling the plasma. Furthermore, as the outer gas has a strong flow rate, the gas layers next to the torch wall stay cool, as is also obvious from Fig. 3 in both cases. The hottest region in the radial direction is close to the middle of the auxiliary gas inlet, which is the place of maximum power deposition (see ref. 23). The absolute values of the calculated plasma temperature, *i.e.* 8000–9000 K above the load coil, are in good agreement with experiments.[1,28]

Insertion of the sampler does not seem to affect the plasma temperature inside the load coil to a great extent. However, a small temperature rise can still be observed, attributed to the change in path lines in this region as seen in Fig. 1. Indeed, in the coil region, when the interface is inserted, the flow originating from the intermediate inlet (path lines colored in black in Fig. 1) passes the area which is characterized by high electrical power deposition (*i.e.*, the center of the purple contours in Fig. 1b), while in the case without sampler, part of the intermediate flow

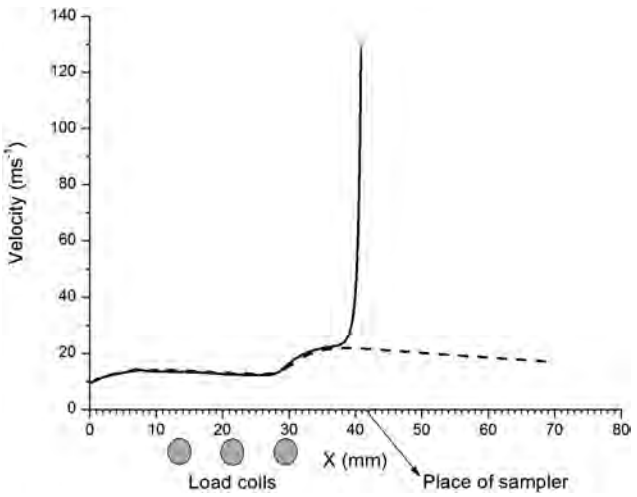

Fig. 2 Axial distribution of gas flow velocity (m s^{-1}) in the case with (solid line) and without (dashed line) the sampler, on the central axis of the plasma torch. The load coils and the place of the sampler are also indicated in this figure, for clarity.

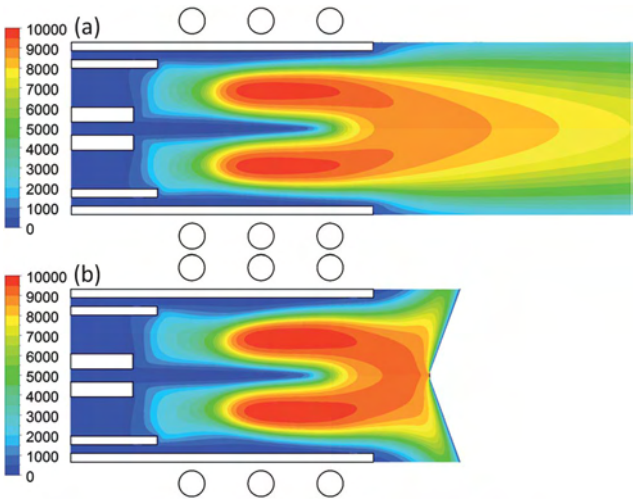

Fig. 3 2D temperature profile (K): (a) without and (b) with the sampler.

passes through the area which has lower coupled power values (see Fig. 1a). The total external power and intermediate mass flow rate are the same in both cases with and without sampler, but the flow seems to pass through more efficient areas to heat up, in the case of the presence of the sampler. In other words, the intermediate flow combines later with the central flow, after passing through the high power area, in the case of the presence of the sampler, while in the other case, part of the intermediate flow combines sooner with the central flow, with less heating by the external power. Therefore, this causes a higher temperature in the central region when the sampler is present, as we will see later in Fig. 5.

To obtain a more detailed picture close to the sampler, which is the most important region for mass spectrometry, Fig. 4 illustrates the plasma temperature distribution in the radial direction, at several axial positions, in the presence and absence of the sampler (*i.e.*, solid and dashed lines, respectively). It is clear that the temperature in the presence of the sampler drops dramatically towards the central axis, with a sharp minimum at about 0.5–1 mm from the central axis, and it is higher again at the central axis. This can be explained by the cooling of the sampler, which has an orifice of 1 mm diameter. It appears from the solid lines in Fig. 4 that the radial temperature profile changes considerably, especially when moving closer towards the sampler. Even at 0.1 mm from the sampler (*i.e.*, solid line in Fig. 4b), the profile looks different from the position of the sampler (*i.e.*, solid line in Fig. 4a), especially near the central axis. This indicates that the above-mentioned cooling effect is only very local. This behavior is important when comparing simulation results with experiments, or different experimental data, *i.e.*, they should be compared at exactly the same position.

Looking at the dashed lines in Fig. 4 tells us that the temperature profile in the case without the sampler is very similar for the different axial positions, with a broad maximum in the central region. Only in Fig. 4e and f a minor local minimum can be observed at the central axis, which arises from the torus-shaped temperature profile in the coil region (see Fig. 3 above). On the other hand, the temperature profile in the presence of a sampler is largely affected by the sampler, and differs a lot for different axial positions, especially near the sampler position, as discussed

above. At the position of the sampler (Fig. 4a) the temperature drops significantly in the central area and it increases in the outer regions, compared to the case without the sampler. Lehn *et al.*[19] have reported the same behavior, but it should be mentioned that the setup of their experiments was different from ours and consequently, they observed a similar behavior but at different positions compared to our work. The drop in the central region was explained above, *i.e.*, it originates from the cooling from the sampler. The higher temperature in the outer regions is attributed to the different path lines, as shown in Fig. 1b above. Indeed, the gas flow which is accelerated to the orifice mostly originates from the central torch inlet, whereas the gas molecules coming from the intermediate and outer torch inlets change their path and leave the ICP torch as they face the interface cone. This affects the temperature profile, as is obvious from Fig. 3b, *i.e.*, the high temperature plasma is spread towards the open sides of the torch, resulting in higher temperature values in the region outside the load coil, at radial positions farther away from the central axis, compared to the case without sampler (Fig. 3a). Therefore, the radial temperature distributions plotted in Fig. 4 exhibit larger values in the outer regions in the case with sampler compared to without. A similar effect as in Fig. 4a is also observed in Fig. 4b, c and d, for the temperature profiles at 9.9 mm, 9.6 mm, and 9.3 mm away from the load coil, respectively, or in other words, 0.1 mm, 0.4 mm, and 0.7 mm from the sampler, respectively, although the cooling effect in the central region is far less pronounced. At positions further away from the sampler (see Fig. 4e and f) the temperature profiles with and without the sampler look very similar, indicating that the sampler does not affect the temperature profile at positions beyond 1 mm from the sampler.

Fig. 5 shows the temperature as a function of axial position on the central axis, again with and without the sampler (*i.e.*, solid and dashed lines, respectively). Note that $x = 0$ mm corresponds to the position of the central gas injector into the ICP. As is obvious from Fig. 3, the temperature at the central axis is very low in the coil region, and it starts to increase dramatically at the end of the coil region. This is also clear from Fig. 5. As the sampler is placed at 41.5 mm from the injector, the solid line stops at this position, while the dashed line continues until 70 mm from the injector. A slightly higher temperature at the central axis is observed in the case with sampler compared to without. This is attributed to the plasma heat conductivity from the slightly higher off-axis plasma temperature in this case, as mentioned above. Moreover, as seen in Fig. 1, the path lines of the central flow in the case with sampler are broader than in the

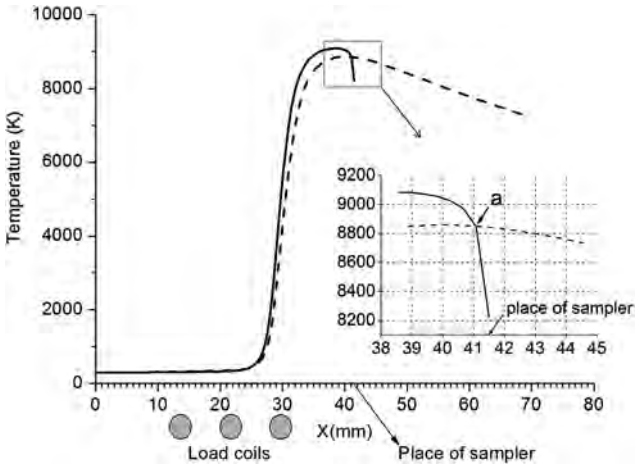

Fig. 5 Axial distribution of plasma temperature (K) in the case with (solid line) and without (dashed line) the sampler, on the central axis of the plasma torch. The load coils and the place of the sampler are also indicated in this figure, for clarity. The small graph shows a detail of the crossing point of the two lines.

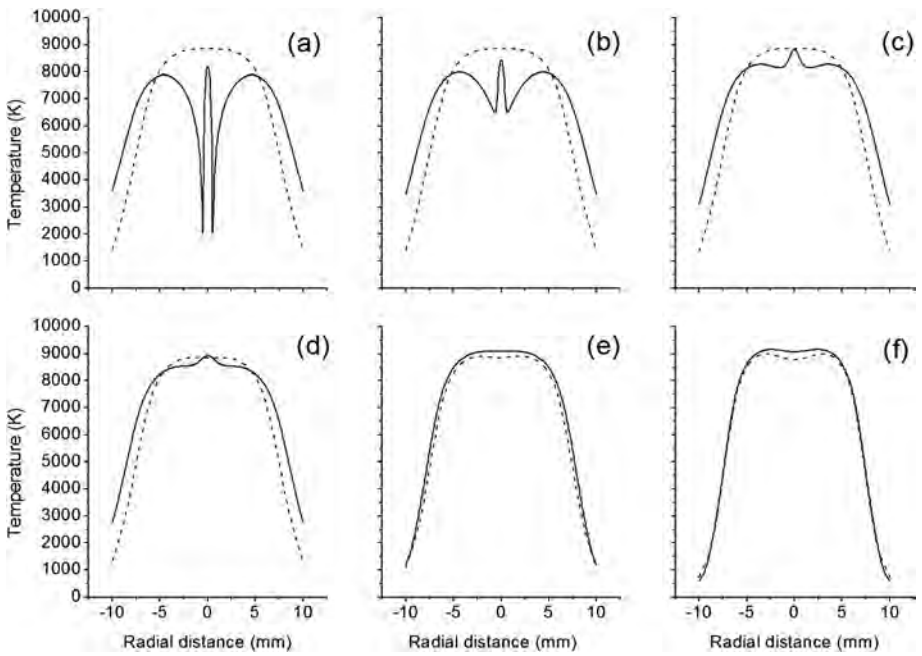

Fig. 4 Radial distributions of plasma temperature (K) in the case with (solid lines) and without (dashed lines) the sampler, at several axial positions, *i.e.*, at 10 mm (place of the sampler) (a), 9.9 mm (b), 9.6 mm (c), 9.3 mm (d), 8 mm (e), and 6 mm (f) from the load coil.

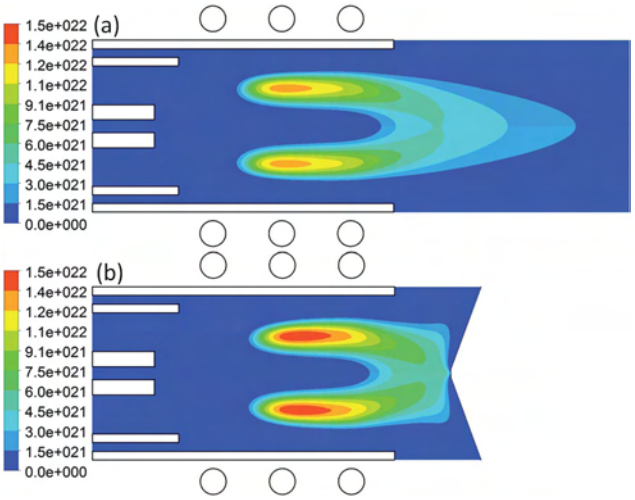

Fig. 6 2D electron density profile (m^{-3}): (a) without and (b) with sampler.

case without the sampler. Therefore, in Fig. 1b, the central path lines come closer to the region of high power coupling, which is another reason for the higher temperature at the central area of the torch. Only close to the sampler, the situation is reversed, and the temperature drops significantly due to the presence of the cooled metal sampler, as is also observed in Fig. 4. This so-called cross-point (point 'a' in Fig. 5) was also reported in ref. 4 from images of ion fluorescence.

3.3. Electron density

Another fundamental property of the ICP is the electron number density, which determines the electrical conductivity in the plasma, as well as the analyte excitation and ionization rates due to electron impact.[29,30]

Fig. 6a and b present the 2D profiles of the electron density, without and with the sampling interface, respectively. Again, the maximum electron density in both cases is reached at the position of maximum power coupling, where also the plasma temperature exhibits its maximum. Moreover, the electron density appears again somewhat higher in the case with the sampler than without (*i.e.*, about 1.5×10^{22} m^{-3} *vs.* 1.3×10^{22} m^{-3}). This can be explained by the slightly higher maximum temperature in the case with the sampler, as mentioned above.

In Fig. 7, the radial distributions of electron density at different axial positions are presented in the case with and without the sampling interface (solid and dashed lines, respectively). In the presence of a sampler, again the measurement position clearly affects the results obtained. At the position of the sampler (10 mm from load coil; solid line in Fig. 7a), the electron density exhibits two maxima at 4–5 mm from the center, and a small one in the center, whereas at 0.1 mm, 0.4 mm and 0.7 mm before the sampler (*i.e.*, solid lines in Fig. 7b–d, respectively), the peak in the center becomes much more pronounced. The general pattern here follows the temperature changes discussed in Section 3.2 above; however, the change in electron density is larger than for the temperature, which can be explained from the temperature dependence in the Saha equation ($n_e \propto T^{3/2}\exp[-(E_i - \Delta E_i)/kT]$, where E_i is the ionization potential, ΔE_i is the ionization potential reduction and k is the Boltzmann constant).[1] The measurements by Lehn *et al.*[19] revealed the same behavior, but because of the different geometries, direct comparison is not possible.

Looking at the dashed lines in Fig. 7 (*i.e.*, calculation results without sampler), it is clear that the profiles do not change a lot for different axial positions, except for the appearance of a small minimum near the center in Fig. 7f, which arises from the two

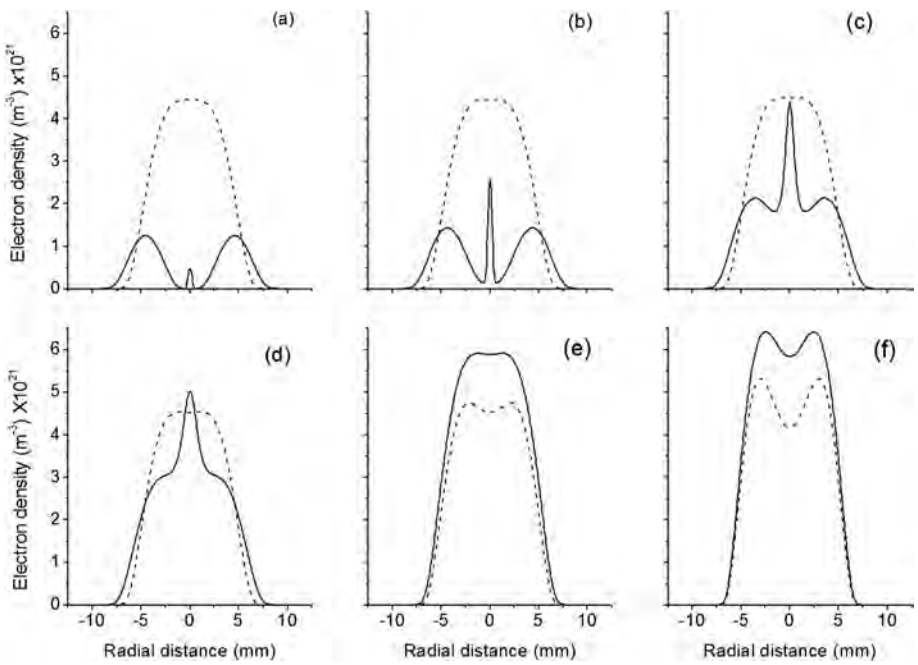

Fig. 7 Radial distributions of electron density (m^{-3}) in the case with (solid lines) and without (dashed lines) the sampler, at 10 mm (place of the sampler) (a), 9.9 mm (b), 9.6 mm (c), 9.3 mm (d), 8 mm (e), and 6 mm (f) from the load coil.

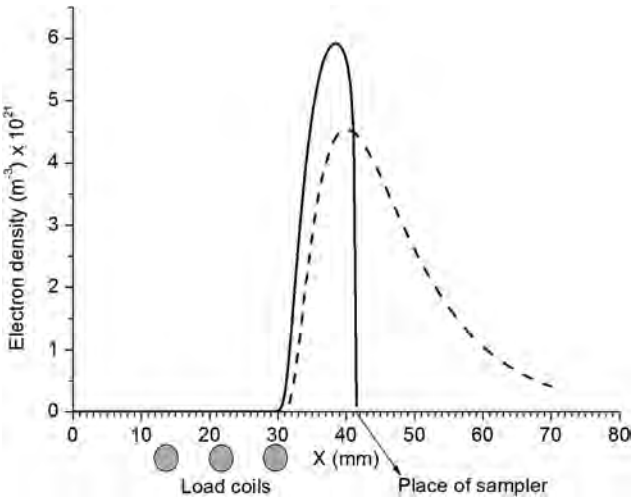

Fig. 8 Axial distribution of electron density (m^{-3}) in the case with (solid line) and without (dashed line) the sampler, on the central axis of the plasma torch. The load coils and the place of the sampler are also indicated in this figure, for clarity.

characteristic maxima observed inside the coil region (see Fig. 6). However, the profiles in the case with sampler are very much dependent on the axial position as discussed above. The closer to the sampler, the larger is the difference between the two profiles. In the case with the sampling interface, the electron density becomes much lower in the central region and somewhat higher in the outer sides, at the position of the sampler (Fig. 7a) as well as at 0.1 mm, 0.4 mm and 0.7 mm away from the sampler (Fig. 7b–d). The drop in density is attributed to the cooling effect of the interface cone in the central region, and the slightly higher density in the outer regions is due to the path lines of the intermediate and outer gas inlets, extending the plasma towards the outer region, as discussed above for the temperature. As these positions are too close to the sampler for accurate measurements, there are no experimental data reported in the literature for these positions. However, further away from the sampler, the electron density appears to be higher, both in the center and in the outer regions, as is clear from Fig. 7e and f (indicating measurement positions of 2 mm and 4 mm from the sampler, respectively).

The latter effect is seen more clearly in Fig. 8, illustrating the axial electron density profile at the center axis, with and without the sampling interface (solid and dashed lines, respectively). Close to the sampler, the electron density is near zero, and hence lower than in the case without the sampler, but it shows a pronounced rise at a few mm from the sampler, and hence, in general the electron density is higher in the case with the sampler than without, due to the slightly higher temperature as explained above. This behavior was also reported by Ma *et al.*,[4] based on ground state ion fluorescence measurements, obtained at positions of 1 mm from the sampler.

4. Conclusion

The effect of a mass spectrometer sampling interface on the fundamental plasma characteristics in an ICP, *i.e.*, gas flow velocity, plasma temperature and electron density, is computationally investigated. The model deals with plasma by kinetic theory in the whole ICP torch region to provide a complete description of ICPMS upstream from the sampler.

The calculation results indicate that the maximum temperature and electron density increase when a sampling cone is inserted in the ICP. Moreover, the plasma velocity increases dramatically when flowing through the sampling orifice, due to the sudden pressure drop. The sampler cools the gas flowing into the MS, which results in a reduction of the total number of ions that can be measured. Thus, maybe an increase of the sampler temperature could yield an increased transmission of ions into the MS. The effect of the sampler is especially important in the downstream region from the plasma, but not so much in the most intense plasma region (*i.e.*, the coil region). Other effects, such as for instance the effect of a nebulizer flow that also contains water, will mainly affect the plasma in the coil region, and the effect close to the sampler will probably be minor.

From the detailed radial profiles of temperature and electron density at different axial positions, it is clear that the changes induced by the sampling cone are very sensitive to the distance from the sampler. The general behavior is a decrease in the central region and a rise in the outer areas for both the temperature and the electron density profiles, close to the sampler. Further away from the sampler, both temperature and electron density are higher than in the case without sampler, also in the central region. These calculations are of great value, because they yield information about the plasma very close to the sampler, *i.e.*, a region which is not or barely accessible by measurements and which is nevertheless the most important plasma region where the measured data are sampled from, as it is the connection point between the ICP and the mass spectrometer.

Acknowledgements

The authors gratefully acknowledge financial support from the Prime Minister's Office through IAP VI. This work was carried out using the Turing HPC infrastructure at the CalcUA core facility of the Universiteit Antwerpen, a division of the Flemish Supercomputer Center VSC, funded by the Hercules Foundation, the Flemish Government (department EWI) and the Universiteit Antwerpen.

References

1 A. Montaser, *Inductively Coupled Plasma Mass Spectrometry*, Wiley, New York, 1998.
2 A. Montaser and D. W. Gologhtly, *Inductively Coupled Plasmas in Analytical Atomic Spectrometry*, VCH Publishers, New York, 1992.
3 J. A. C. Broekaert, *Analytical Atomic Spectrometry with Flames and Plasmas*, Wiley, Weinheim, 2005.
4 H. Ma, N. Taylor and P. B. Farnsworth, The effect of the sampling interface on spatial distributions of barium ions and atoms in an inductively coupled plasma ion source, *Spectrochim. Acta, Part B*, 2009, **64**, 384–391.
5 *Inductively Coupled Plasma Spectrometry and Its Applications*, ed. S. J. Hill, CRC Press, Boca Raton, 1999.
6 B. S. Duersch and P. B. Farnsworth, Characterization of the ion beam inside the skimmer cone of an inductively coupled plasma mass spectrometer by laser excited atomic and ionic fluorescence, *Spectrochim. Acta, Part B*, 1999, **54**, 545–555.
7 D. M. Chambers and G. M. Hieftje, Fundamental studies of the sampling process in an inductively coupled plasma mass spectrometer. II. Ion kinetic energy measurements, *Spectrochim. Acta, Part B*, 1991, **46**, 761–784.

8 A. L. Gray, R. S. Houk and J. G. Williams, Langmuir probe potential measurements in the plasma and their correlation with mass spectral characteristics in inductively coupled plasma mass spectrometry, *J. Anal. At. Spectrom.*, 1987, **2**, 13–20.

9 R. S. Houk, J. K. Schoer and J. S. Crain, Plasma potential measurements for inductively coupled plasma mass spectrometry with a center-tapped load coil, *J. Anal. At. Spectrom.*, 1987, **2**, 283–286.

10 I. I. Stewart, C. E. Hensman and J. W. Olesik, Influence of gas sampling on analyte transport within the ICP and ion sampling for ICP-MS studied using individual, isolated sample droplets, *Appl. Spectrosc.*, 2000, **54**, 164–174.

11 G. Meyer, R. Foster, A. Van der Hoeff, T. Albert, S. Luan, K. Hu, S. Karpova-Nadel and J. Schmeizel, Increasing laboratory productivity by combining ICP optical emission with ICP mass spectrometry, *Am. Lab.*, 1996, **28**, 21–24.

12 H. P. Longerich, Mass spectrometric determination of the temperature of an argon inductively coupled plasma from the formation of the singly charged monoxide rare earths and their known dissociation energies, *J. Anal. At. Spectrom.*, 1989, **4**, 491–497.

13 K. Lepla, M. A. Vaughan and G. Horlick, Simultaneous atomic emission and mass spectrometric measurements on an inductively coupled plasma, *Spectrochim. Acta, Part B*, 1991, **46**, 967–973.

14 R. S. Houk and Y. Zhai, Comparison of mass spectrometric and optical measurements of temperature and electron density in the inductively coupled plasma during mass spectrometric sampling, *Spectrochim. Acta, Part B*, 2001, **56**, 1055–1067.

15 R. S. Houk, J. K. Schoer and J. S. Crain, Deduction of excitation temperatures for various analyte species in inductively coupled plasmas from vertically-resolved emission profiles, *Spectrochim. Acta, Part B*, 1987, **42**, 841–852.

16 L. Pei-Qi, G. Pei-Zhing, L. Tei-Zheng and R. S. Houk, Langmuir probe measurements of electron temperature in an ICP, *Spectrochim. Acta, Part B*, 1988, **43**, 273–285.

17 H. Niu and R. S. Houk, Fundamental aspects of ion extraction in inductively coupled plasma mass spectrometry, *Spectrochim. Acta, Part B*, 1996, **51**, 779–815.

18 J. S. Crain, F. G. Smith and R. S. Houk, Mass spectrometric measurement of ionization temperature in an inductively coupled plasma, *Spectrochim. Acta, Part B*, 1990, **45**, 249–259.

19 S. A. Lehn, K. A. Warner, M. Huang and G. M. Hieftje, Effect of an inductively coupled plasma mass spectrometry sampler interface on electron temperature, electron number density, gas-kinetic temperature and analyte emission intensity upstream in the plasma, *Spectrochim. Acta, Part B*, 2002, **57**, 1739–1751.

20 R. L. Spencer, J. Krogel, J. Palmer, A. Payne, A. Sampson, W. Somers and C. N. Woods, Modeling the gas flow upstream and in the sampling nozzle of the inductively coupled plasma mass spectrometer *via* the Direct Simulation Monte Carlo algorithm, *Spectrochim. Acta, Part B*, 2009, **64**, 215–221.

21 R. L. Spencer, N. Taylor and P. B. Farnsworth, Comparison of calculated and experimental flow velocities from the sampling cone of an inductively coupled plasma mass spectrometer, *Spectrochim. Acta, Part B*, 2009, **64**, 921–924.

22 D. J. Douglas and J. B. French, Gas dynamics of the inductively coupled plasma mass spectrometry interface, *J. Anal. At. Spectrom.*, 1988, **3**, 743–747.

23 H. Lindner and A. Bogaerts, Multi-element model for the simulation of inductively coupled plasmas: effects of helium addition to the central gas stream, *Spectrochim. Acta, Part B*, 2011, **66**, 421–431.

24 H. Lindner, A. Murtazin, S. Groh, K. Niemax and A. Bogaerts, Simulation and experimental studies on plasma temperature, flow velocity and injector diameter effects for an inductively coupled plasma, *Anal. Chem.*, **83**, 9260–9266.

25 Ansys Fluent 12.0/12.1 Documentation.

26 P. Yang, J. A. Horner, N. N. Sesi and G. M. Hieftje, Comparison of simulated and experimental fundamental ICP parameters, *Spectrochim. Acta, Part B*, 2000, **55**, 1833–1845.

27 J. A. Horner and G. M. Hieftje, Computerized simulation of mixed-solute-particle vaporization in an inductively coupled plasma, *Spectrochim. Acta, Part B*, 1998, **53**, 1235–1259.

28 Y. Nojiri, K. Tanabe, H. Uchida, H. Haraguchi, K. Fuwa and J. D. Winefordner, Comparison of spatial distribution of argon species number densities with calcium atom and ion in an inductively coupled argon plasma, *Spectrochim. Acta, Part B*, 1983, **38**, 61–74.

29 N. N. Sesi, D. S. Hanselman, P. Galley, J. Horner, M. Huang and G. M. Hieftje, An imaging-based instrument for fundamental plasma studies, *Spectrochim. Acta, Part B*, 1997, **52**, 83–102.

30 M. Huang and G. M. Hieftje, Simultaneous measurement of spatially resolved electron temperatures, electron number densities and gas temperatures by laser light scattering from the ICP, *Spectrochim. Acta, Part B*, 1989, **44**, 739–749.

